

2. OPERATION PRINCIPLES

2.1. Converter Operation

Control of the converter in Fig. 1.2 is derived from a combination of three techniques. First, the SVM technique [10, 28, 32] is adopted for the synthesis of the bridge ac voltages because it provides the best possible voltage gain, the smallest ac current ripple with the lowest number of switching actions, the least amount of high-frequency circulating energy [26], and inherent suitability for transient operation. Second, the SVM algorithm is modified to allow synchronized turn-on of all bridge switches under any conditions so that the ZVT technique described in [4] can be applied. Third, the ac currents are regulated by using two current controllers in a rotating reference frame [26, 30].

2.2. Space Vector Modulation

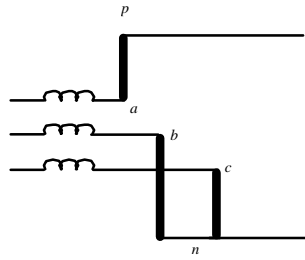
Due to topological restrictions, the main bridge of the converter in Fig. 1.1 may assume only eight switching combinations, *i.e.* a path must be provided for the main inductor currents and no short circuit must be applied to the dc side capacitor. Therefore, one and only one connection is made in each leg of the bridge at a time. Those switching combinations are shown in Fig. 2.1. From the

latter it is clear that only six of these switching combinations, Fig. 2.1(a)-(f), yield non-zero voltage between nodes a , b , c and the other two combinations, Fig. 3(g)-(h), yield zero voltage. In the space vector representation [10], these combinations, a - f , correspond to the six non-zero discrete voltage vectors, V_{pnn} , V_{ppn} , V_{nnp} , V_{npp} , V_{nnp} , and V_{pnp} , and the two zero voltage vectors V_{ppp} and V_{nnn} , as shown in Fig. 2.2(a). Inspection of Fig. 2.1 and 2.2 reveals that the subscript letters represent the circuit state; for example V_{pnn} corresponds to the state in which node a is connected to the positive rail p while nodes b and c are connected to the negative rail n . These vectors, also called the switching state vectors (SSVs), form the SVM hexagon which is divided into six sectors. Each sector is defined by two non-zero vectors whose node voltages differ in only one position, *e.g.* V_{pnn} and V_{ppn} .

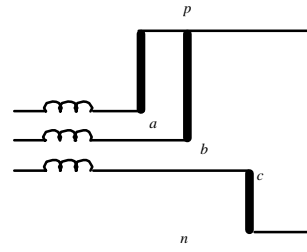
In SVM [10, 28, 32], the rotating reference space vector of desired line voltages V_r , is synthesized at any given instant by PWM of its two adjacent SSVs and a zero vector. For the example in Fig. 2.2(b) V_r is in sector II and it can be synthesized as

$$V_r = d_1 \cdot V_{pnn} + d_2 \cdot V_{ppn} + d_0 \cdot V_0 , \quad (2.1)$$

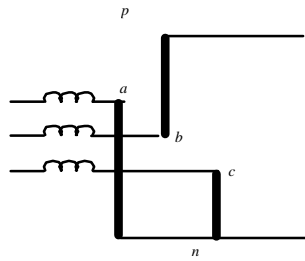
where d_1 and d_2 are duty-cycles of the SSVs V_{pnn} and V_{ppn} , respectively, and



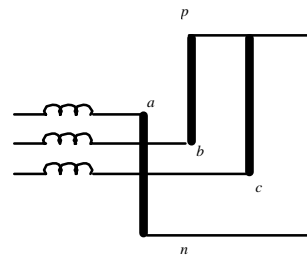
(a) SSV V_{pnn}



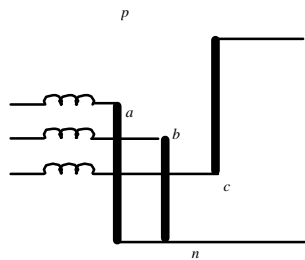
(b) SSV V_{ppn}



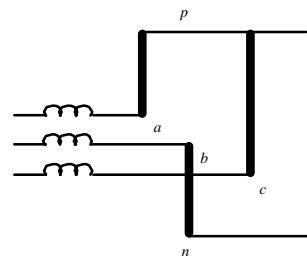
(c) SSV V_{npn}



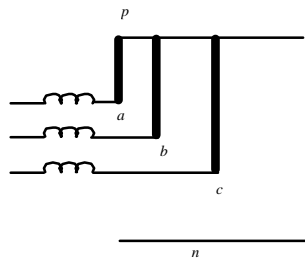
(d) SSV V_{npp}



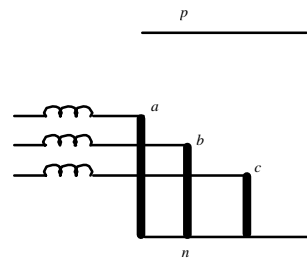
(e) SSV V_{ppp}



(f) SSV V_{pnp}



(g) SSV V_{ppp}



(h) SSV V_{nnn}

Fig. 2.1 Converter Switching States.

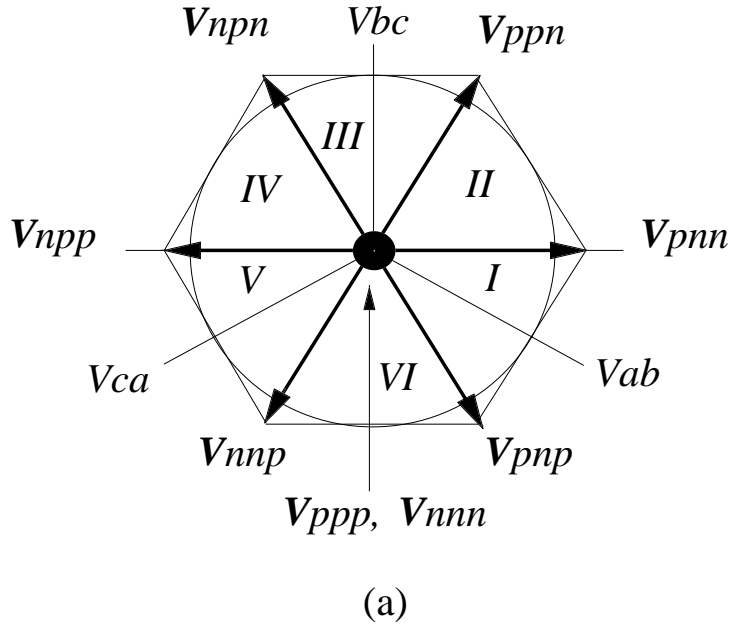
$$d_0 = 1 - d_1 - d_2 \quad (2.2)$$

is the duty-cycle of the zero SSV, V_{ppp} or V_{nnn} .

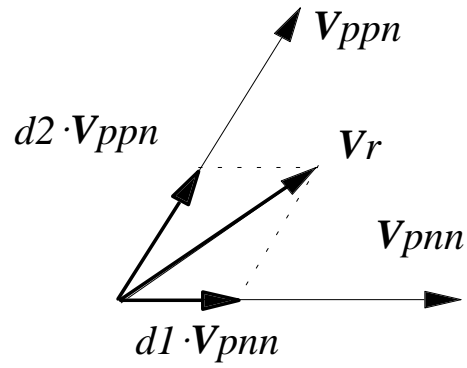
The sequence in which the SSVs are generated within a switching cycle does not affect the value of the reference vector \mathbf{V}_r . However, the fact that the commutation circuit in Fig. 1.2 provides zero-voltage turn-on for the switches and soft turn-off for the diodes requires the sequence to be modified so that the currents are commutated from the diodes only once per switching cycle. Then, a single auxiliary circuit intervention (AUXI) can turn-off all the conducting diodes and turn-on all the necessary switches.

2.3. Auxiliary Intervention.

Assume that at a given instant the three-phase currents in Fig. 1.2 satisfy $i_a > 0$, $0 > i_b > i_c$, and that the currents flow through the diodes D_{ap} , D_{bn} and D_{cn} , even though their anti-parallel switches, S_{ap} , S_{bn} , and S_{cn} are closed. The goal is to commutate the currents from the diodes D_{ap} , D_{bn} , and D_{cn} to switches S_{an} , S_{bp} and S_{cp} while achieving ZVS for all the switches and diodes involved in the transition. This is achieved by activating the auxiliary circuit for a short duration around the commutation instant.



(a)



(b)

Fig. 2.2 SVM hexagon and vector addition.

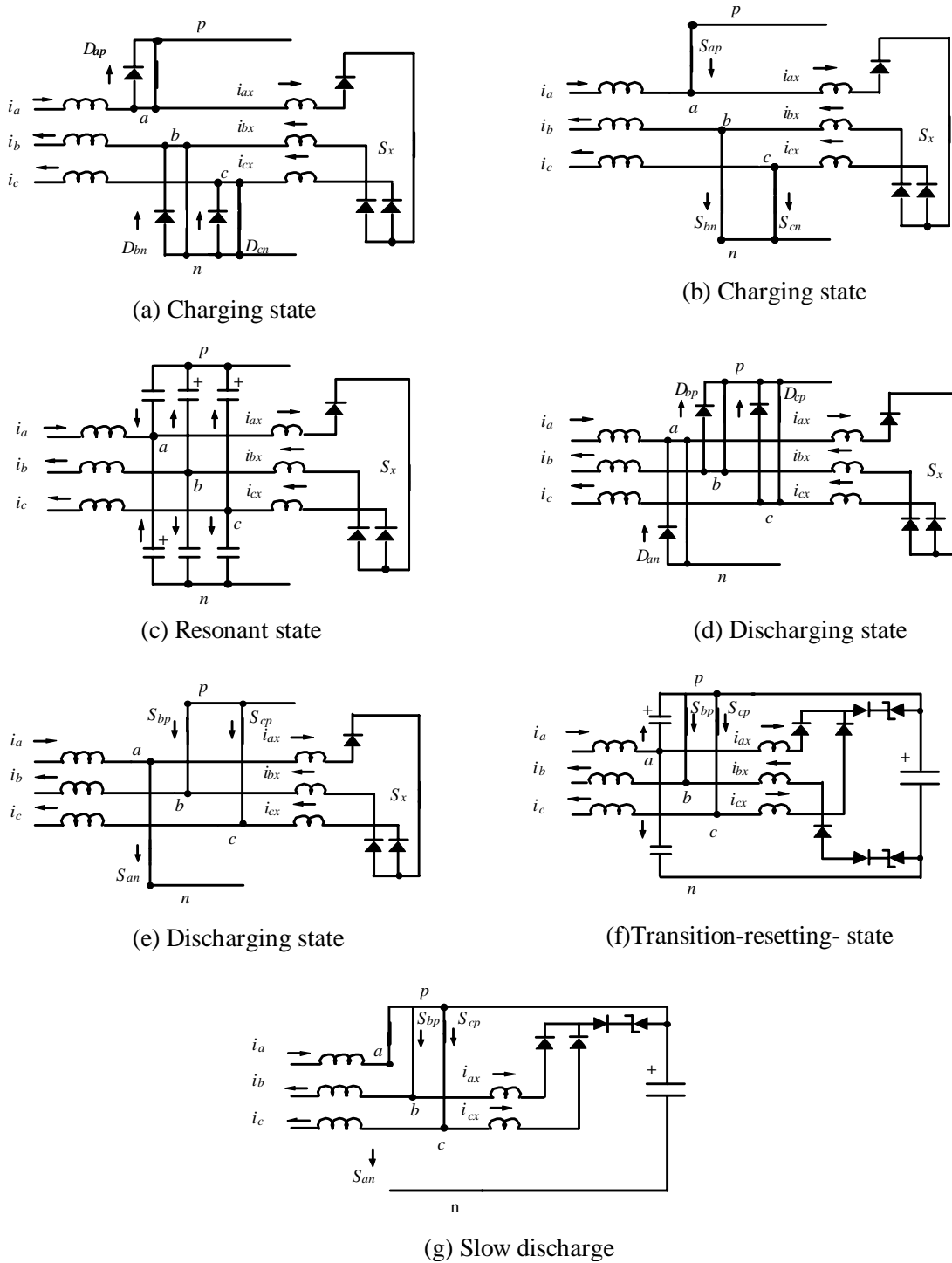


Fig. 2.3 Topological sequence of one auxiliary intervention (Rec.).

The topological sequence of the resulting circuit during the auxiliary intervention (AUXI) in the rectifier mode of operation is shown in Fig. 2.3. The corresponding experimental waveforms are shown in Fig. 2.4. The AUXI starts at t_1 by closing the auxiliary switch S_x which places the circuit into the charging state shown in Fig. 2.3(a). The auxiliary inductor currents i_{ax} , i_{bx} , and i_{cx} , increase linearly until they exceed the currents i_a , i_b , and i_c , respectively, when the diodes D_{ap} , D_{bn} , and D_{cn} are softly turned-off and the switches S_{ap} , S_{bn} , and S_{cn} start conducting, Fig 2.3(b). The bumps in the node voltage waveforms during the charging state represent the change into conduction for the main switches, *i.e.* IGBTs, and the situation arises when their $|di/dt|$ is too large. The AUXI continues with the auxiliary inductors being charged until the switches S_{ap} , S_{bn} , and S_{cn} are simultaneously turned-off at t_2 . This action transfers the circuit into the resonance state shown in Fig. 2.3(c) in which the auxiliary inductors resonate with the node parasitic and snubbing capacitances since the main inductors are assumed to be much larger than the auxiliary inductors ($L_f \gg L_x$). The node voltages smoothly change until they reach the opposite rail at t_3 . At this moment the diodes D_{an} , D_{bp} , and D_{cp} turn-on, and the circuit is transferred into the discharging state shown in Fig. 2.3(d). Now the switches S_{an} , S_{bp} , and S_{cp} can be turned-on under zero-voltage condition. The voltage across the auxiliary inductors is reversed causing the auxiliary currents to discharge linearly until they become smaller than the main

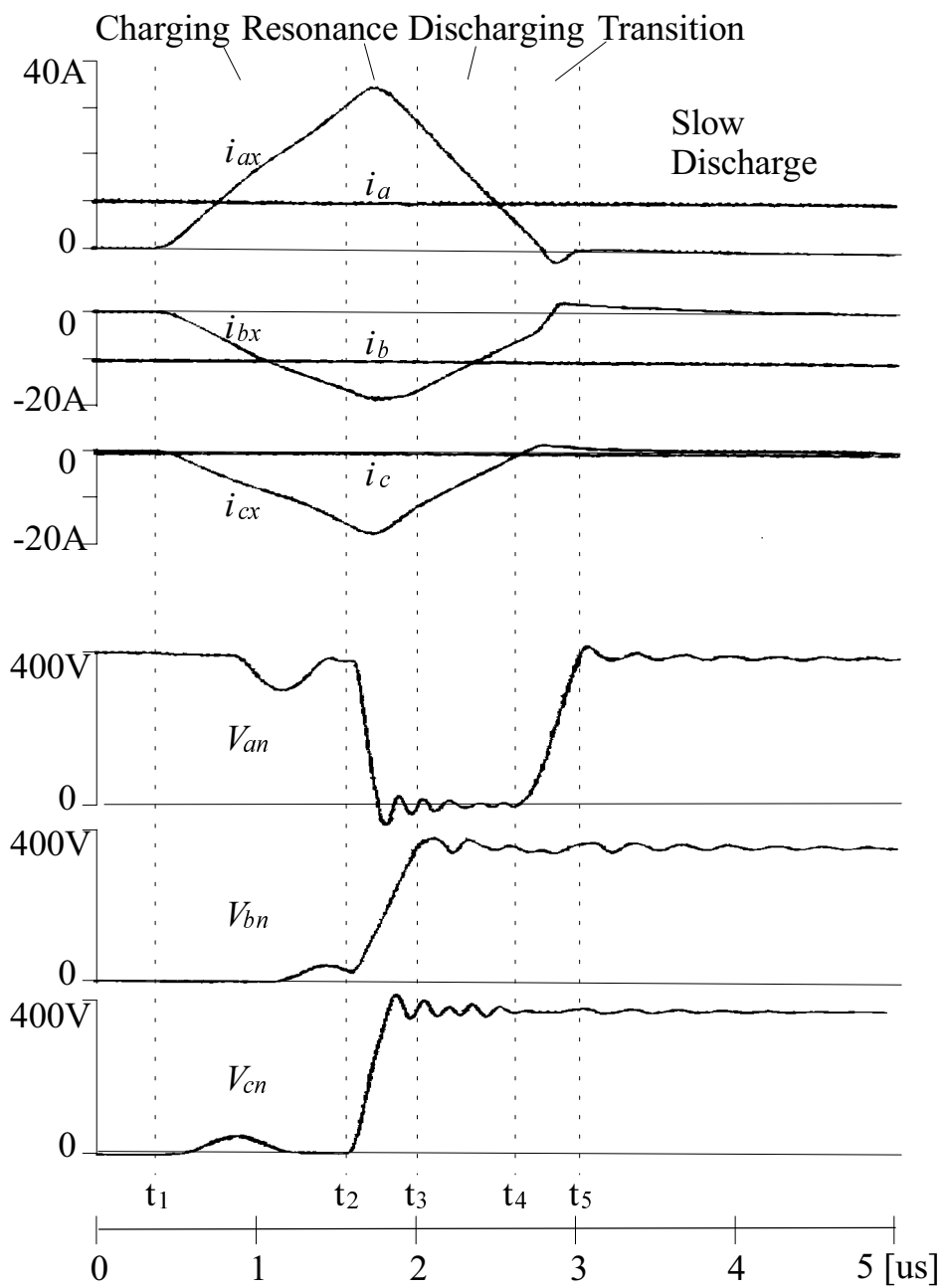


Fig. 2.4 Experimental high frequency waveforms in rectifier mode.

currents, when the switches begin conducting, Fig. 2.3(e). Switch S_x remains on until the current i_{cx} reduces to zero. At this time S_x and S_a are turned-off which marks the end of AUXI.

The opening of S_x , at t_4 in Fig. 2.3, leads to a short secondary resonance between the auxiliary inductors and the parasitic capacitances across S_x , and then to a resetting state where the full dc voltage, V_{pn} , is applied across auxiliary inductor b , which shows as a steeper slope in i_{bx} . At the same time the opening of S_a , allows for the transition of node-voltage a from rail n to rail p , Fig. 2.3(f). Upon completion of this transition the circuit goes to the state shown in Fig. 2.3(g) where the energy remaining in the auxiliary inductors is dissipated in the series connection of a main switch, two rectifier diodes and a zener diode. This is seen as the slow decay of i_{bx} and i_{cx} after t_5 in Fig. 2.4.

The AUXI sequence during the inverter mode of operation is explained next. Assume that at a given instant the same situation as in the example above exists, *i.e.* the three-phase currents satisfy $i_a > 0$, $i_b < 0$, and $i_c < 0$, and the main bridge produces the SSV V_{pnn} . The currents flow through the diodes D_{ap} , D_{bn} and D_{cn} , even though their anti-parallel switches are on. Figures 2.5 and 2.6 show the topological sequence of the resulting AUXI and the corresponding experimental waveforms respectively. The AUXI starts at t_1 by closing the auxiliary switch S_x .

This places the circuit into the charging state shown in Fig. 2.5(a). The auxiliary inductor currents i_{ax} , i_{bx} , and i_{cx} , increase linearly until they exceed the currents i_a , i_b , and i_c , respectively, when the diodes D_{ap} , D_{bn} , and D_{cn} are softly turned-off and the switches S_{ap} , S_{bn} , and S_{cn} start conducting, Fig 2.5(b). The auxiliary inductors continue charging until the switches S_{ap} , S_{bn} , and S_{cn} are simultaneously turned-off at t_2 . This transfers the circuit into the resonant state shown in Fig. 2.5(c) in which the auxiliary inductors ($L_f \gg L_x$) resonate with the node parasitic and snubbing capacitances. The node voltages smoothly change until they reach the opposite rail at t_3 . At this instant the diodes D_{an} , D_{bp} , and D_{cp} turn-on, the circuit is transferred into the discharging state shown in Fig. 2.5(d), and the switches S_{an} , S_{bp} and S_{cp} are turned-on under zero-voltage condition. The voltage across the auxiliary inductors is reversed causing the auxiliary currents to discharge linearly until they become smaller than the main currents, when the switches will begin conducting, Fig. 2.5(e). Switch S_x remains on until the current i_{bx} reduces to zero.

The opening of S_x at t_4 in Fig. 2.4 leads to a secondary resonance between the auxiliary inductors and the parasitic capacitances across S_x , Fig. 2.5(f). After the parasitic capacitances have been charged, the circuit enters the resetting state shown in Fig. 2.5(g).

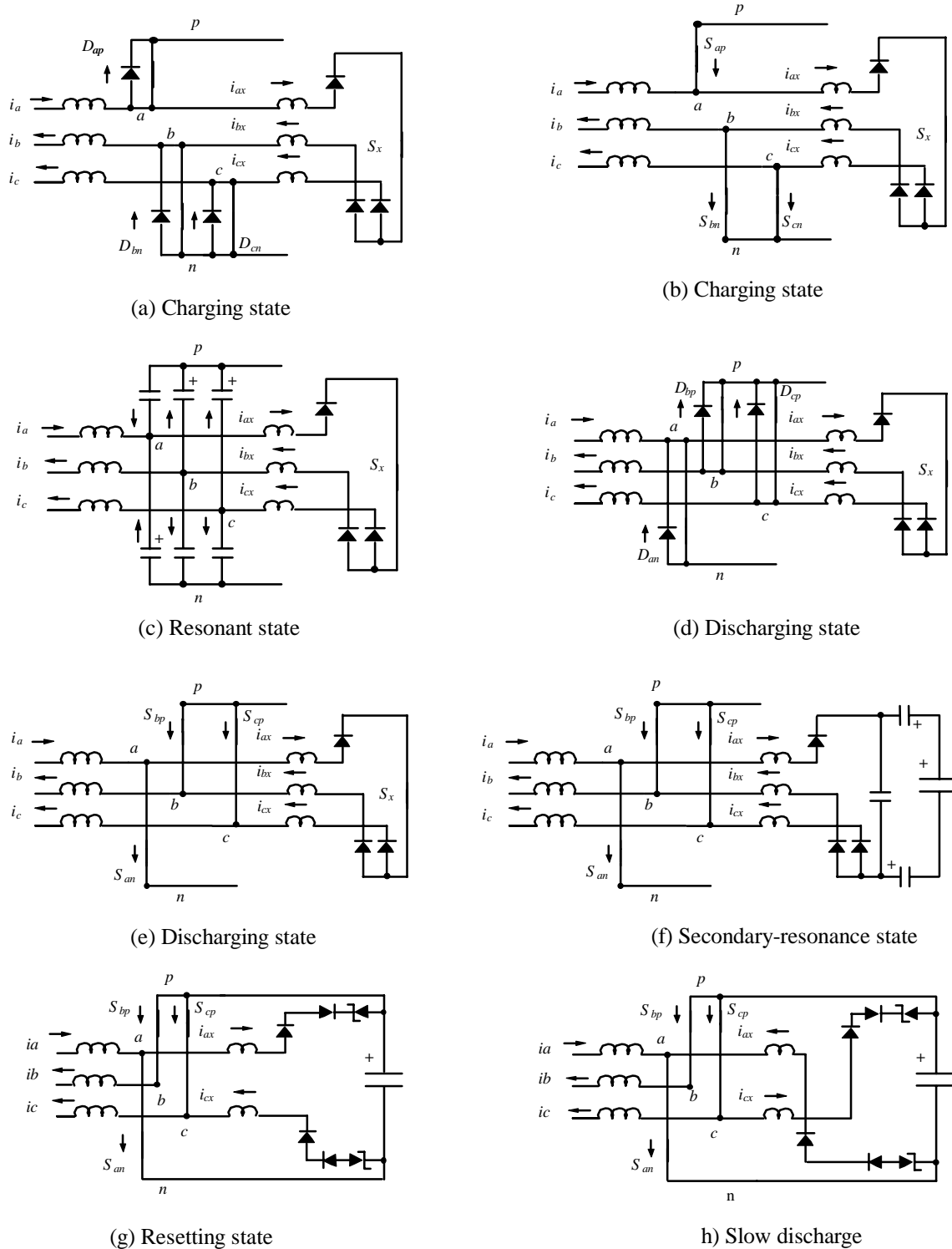


Fig. 2.5 Topological sequence of one auxiliary intervention (Inv.).

The currents i_{ax} and i_{cx} decrease very fast because the full dc voltage, V_{pn} , now appears across the auxiliary inductors. At the end of this state, another short resonance between the auxiliary inductors and the parasitic capacitances of the auxiliary diode bridge occurs and cause the reversal of the currents i_{ax} and i_{cx} . As a result the circuit goes into the state shown in Fig. 2.5(h) where the energy remaining in the auxiliary inductors is dissipated in the series connection of a main switch, two rectifier diodes and a zener diode. This is seen as the slow decay of i_{ax} and i_{cx} after t_5 in Fig. 2.6.

It is important to note that the node voltages at the end of the AUXI are always connected to the opposite rail from where they started, *i.e.* the SSVs at the beginning and the end of the AUXI are always complementary. Because an AUXI always starts from the circuit state in which three diodes are conducting, it always ends in the state in which three switches conduct the main currents.

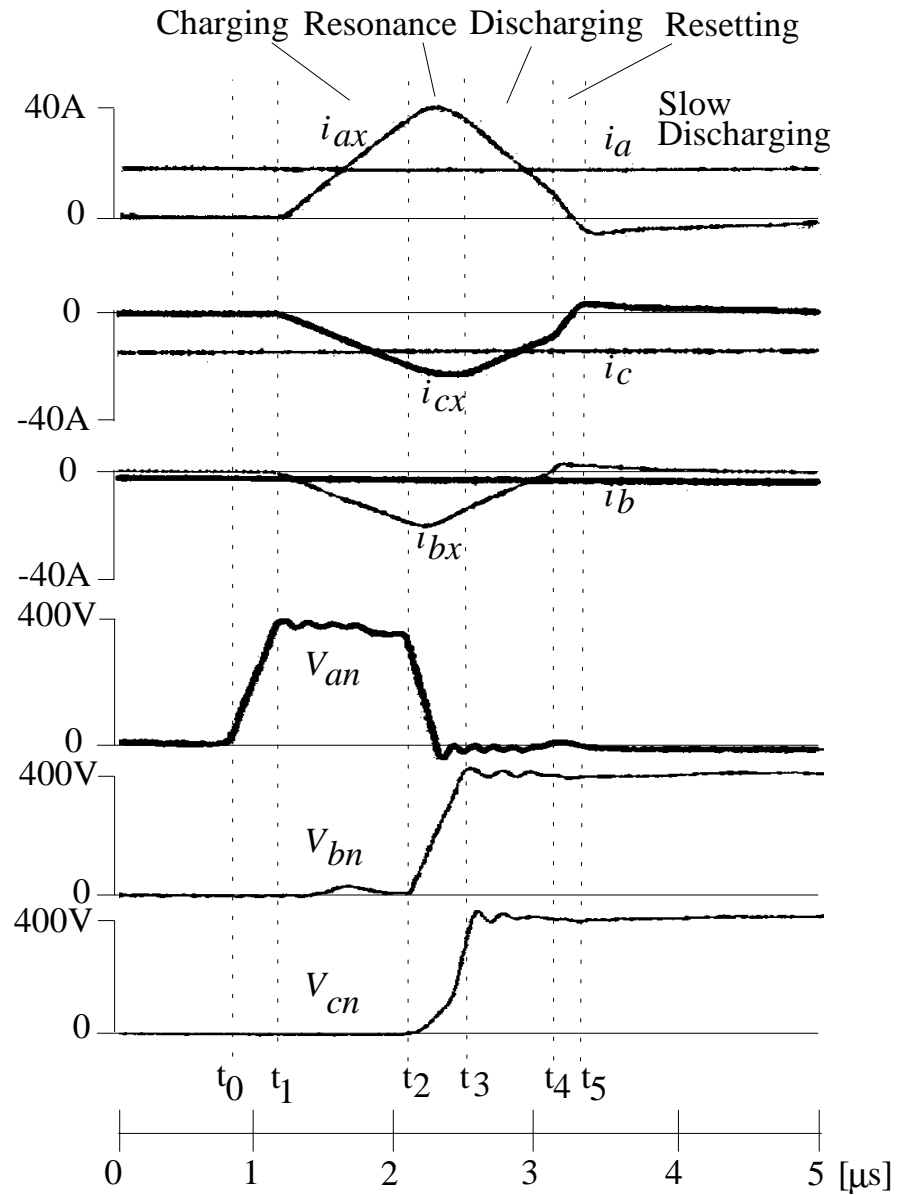


Fig. 2.5 Experimental high frequency waveforms in inverter mode.